Transition Metal Chemistry
https://doi.org/10.1007/s11243-018-0215-7

A green synthesis of biaryls in water catalyzed by palladium nanoparticles immobilized on *N*-amidinoglycine-functionalized iron oxide nanoparticles

Fatemeh Rafiee[1] · **Nasrin Mehdizadeh**[1]

Received: 9 December 2017 / Accepted: 2 February 2018

Abstract
Fe_3O_4 nanoparticles were prepared by co-precipitation and coated with SiO_2 following the Stöber process. *N*-Amidinoglycine amino acid was then covalently connected to provide an excellent ligand for the immobilization of Pd nanoparticles. The resulting material was characterized by FE-SEM, TEM, EDX, XRD, VSM and ICP-AES analysis. The Fe_3O_4@SiO_2@*N*-amidinoglycine@Pd^0 proved to be a highly active catalyst for the Suzuki coupling reactions of various aryl halides with substituted phenylboronic acids in water, giving the desired products in excellent yields for short reaction times. Moreover, this catalyst can be easily recovered by using an external magnet and directly reused for several times without significant loss of activity.

Introduction

Magnetic nanoparticles are of great interest in the field of catalysis [1–3], biotechnology and biomedical applications such as drug delivery, MRI contrast agents and cancer therapy [4–8]. Magnetic nanoparticles with good stability and ready availability can effectively improve the loading and catalytic efficiency of immobilized catalysts, due to their high surface-to-volume ratios. In terms of recycling expensive catalysts, immobilization of these active species on magnetic nanoparticles leads to facile and quick magnetic separation without the need for filtration, centrifugation or other workup processes [9, 10]. However, surface oxidation and agglomeration of chemically highly active naked magnetic nanoparticles can result in a significant decrease in their magnetic properties, dispersibility, surface area and catalytic activity [11]. Given the strong surface affinity of magnetic nanoparticles toward silica as a chemically inert material with high surface area and good stability, it is often employed as coating layer over the surface of magnetic nanoparticles. This surface modification can weaken the particle–particle magnetic bipolar interactions and protect the nanoparticles from aggregation and oxidation processes. Moreover, silica coating not only stabilizes the nanoparticles, but can also be readily functionalized with amines, carboxyls, thiols and biological species [12, 13]. The Stöber method and sol–gel processes are the preferred choices for the coating of magnetic nanoparticles with silica [14–16].

The low cost, good biocompatibility and range of available functional groups of amino acids as capping ligands for magnetic nanoparticles make them an attractive candidate for both coating and surface functionalization. Amino acids interact with the nanoparticle's surface through their carboxyl groups, while their side chains containing various surfaced-exposed functional groups are available. Available amino acid functional groups include guanidine, thiol and phenolic hydroxyl groups, which are potential reaction sites for further modification [17–19].

The palladium-catalyzed Suzuki cross-coupling of organic halides with boronic acids is one of the most versatile methods for the synthesis of biaryls [20]. Biaryls are of significant current interest for the synthesis of biologically active compounds, natural products, macrocycles, liquid-crystal materials and asymmetric catalysts [21–24]. The increasing need for greener synthetic methodologies has led to a growing interest in the development of catalysis that can operate in aqueous medium. The stability of boronic

Electronic supplementary material The online version of this article (https://doi.org/10.1007/s11243-018-0215-7) contains supplementary material, which is available to authorized users.

✉ Fatemeh Rafiee
f.rafiee@alzahra.ac.ir

[1] Department of Chemistry, Faculty of Physic-Chemistry, Alzahra University, Vanak, Tehran, Iran

Published online: 16 March 2018

acids in aqueous solvent is viewed as an advantage of Suzuki coupling compared to other cross-coupling reactions. Recent reviews have covered the literature on palladium-catalyzed Suzuki cross-coupling reactions in water [25, 26].

In this paper, we report the synthesis and characterization of a palladium nanocatalyst based on Fe_3O_4@SiO_2 functionalized with *N*-amidinoglycine amino acid, and its activity in Suzuki cross-coupling reactions.

Results and discussion

Preparation and characterization of the nanocatalyst

The magnetic nanoparticle-supported Pd catalyst designated as Fe_3O_4@SiO_2@*N*-amidinoglycine@Pd^0 was synthesized via multiple steps. The first step was to prepare Fe_3O_4 nanoparticles from $FeCl_3{\cdot}6H_2O$ to $FeCl_2{\cdot}4H_2O$ [27]. The magnetic nanoparticles (MNPs) so obtained were subsequently coated with silica (Fe_3O_4@SiO_2) through the well-known Stöber method, using tetraethylorthosilicate (TEOS) [14]. The Fe_3O_4@SiO_2 core/shell structure was then sequentially treated with *N*-amidinoglycine to form Fe_3O_4@SiO_2@*N*-amidinoglycine. Finally, Pd nanoparticles were immobilized on this support by reaction with $Pd(OAc)_2$ in ethanol, such that Pd^{II} was reduced to Pd^0 without the addition of any external reducing agent (Scheme 1).

The catalyst was subjected to microanalysis, and the proportions of carbon, hydrogen and nitrogen by weight were found to be 1.90, 0.73 and 0.79%, respectively. From the N content, the loading of *N*-amidinoglycine was calculated as 0.19 mmol/g. The amount of palladium in the catalyst, as determined by inductively coupled plasma atomic emission spectroscopy (ICP-AES), was 1.7 mmol/g.

Figure S1 shows the FT IR spectra of Fe_3O_4, Fe_3O_4@SiO_2, Fe_3O_4@SiO_2@*N*-amidinoglycine, palladium

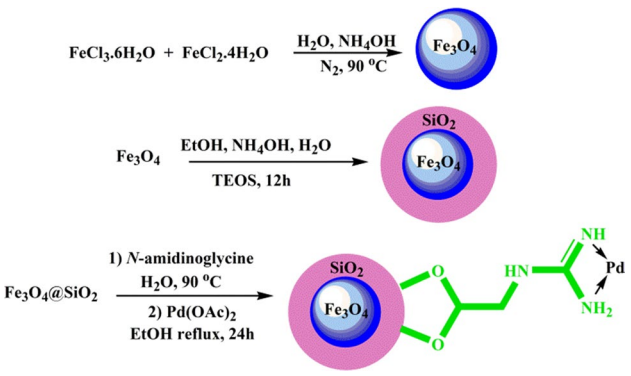

Scheme 1 Procedure for preparation of the Fe_3O_4@SiO_2@*N*-amidinoglycine@Pd^0 Catalyst

supported on this functionalized support, and pure *N*-amidinoglycine. In the spectrum of Fe_3O_4 nanoparticles, a band at 584 cm^{-1} is assigned to the Fe–O bond stretches, and a peak at 3421 cm^{-1} is attributed to the –OH groups. The spectrum of Fe_3O_4@SiO_2 showed a strong absorption band at 1091 cm^{-1}, related to Si–O–Si antisymmetric stretching vibrations; peaks at 799 and 464 cm^{-1} are assigned to the Si–O–Si symmetric stretching and Si–O–Si and or O–Si–O bending modes, respectively. These data confirm the successful coating of silica layers on the Fe_3O_4. Comparisons of the spectra of Fe_3O_4@SiO_2@*N*-amidinoglycine with those of pure amidinoglycine (3384 cm^{-1} (ν_{N-H} of the guanidino group), 3303 and 3172 cm^{-1} (ν_{as} and ν_s of primary amines), 1670 cm^{-1} ($\nu_{C=N}$ of the guanidino group), 1581 and 1411 cm^{-1} (ν_{as} and ν_s of the carboxylate group)) and Fe_3O_4@SiO_2 all indicate successful functionalization of the surface of Fe_3O_4@SiO_2 nanoparticles with *N*-amidinoglycine (Fig. S1d).

In the powder XRD pattern of the catalyst (Fig. S2b), the diffraction peaks observed at $2\theta = 30.14$, 35.50, 43.07, 53.03, 57.11 and 62.74° correspond, respectively, to the crystalline planes (220), (311), (400), (422), (511) and (440) of Fe_3O_4, with a cubic spinel structure. The XRD pattern of the nanocatalyst also showed additional peaks at 39.10, 44.57 and 66.29° which are indexed, respectively, to the (111), (200) and (220) crystalline planes of Pd nanocrystals, suggesting the formation of metallic Pd NPs (Pd^0). Comparison of the spectrum of Fe_3O_4@SiO_2@*N*-amidinoglycine@Pd^0 with that of pure *N*-amidinoglycine (Fig S2a) indicates successful immobilization of this amino acid derivative on the surface of the Fe_3O_4@SiO_2 nanoparticles.

To evaluate the chemical oxidation state of palladium in the catalyst, X-ray photoelectron spectroscopy (XPS) was performed (Fig. S3). The resulting spectrum showed an intense doublet at a binding energy (BE) of 335.7 and 340.8 eV related to Pd^0, assigned to the Pd $3d_{5/2}$ and Pd $3d_{3/2}$ peaks, respectively. This observation confirmed the successful reduction of Pd^{II} to Pd^0 in the process of catalyst preparation. An XPS elemental survey scan of the surface of the nanocatalyst also revealed the presence of Fe (Fe 2p at binding energies of 711.08 and 724.08 eV), O (O 1s at binding energies of 530.58 and 532.98 eV), Si (Si 2p at binding energy of 103.08 eV and Si 2s at 154.08 eV), N (N 1s at 399.88 eV) and C (C 1s at 284.78 and 288.48 eV).

The magnetic properties of the nanocatalyst were investigated with a vibrating sample magnetometer (VSM) at room temperature in an applied magnetic field sweeping from − 10 to 10 kOe (Fig. S4). The magnetization curves of the prepared catalyst exhibit no hysteresis loop, indicating superparamagnetic behavior. The saturation magnetization (M_s) value for the Fe_3O_4@SiO_2@*N*-amidinoglycine@Pd^0 catalyst (23.35 emu g^{-1}) is lower than that of bare Fe_3O_4 due to the successful grafting of SiO_2 and *N*-amidinoglycine@

Pd^0 on the surface of the Fe_3O_4 nanoparticles. The magnetic properties of the silica coated magnetic samples depend on the Fe_3O_4 content. The non-magnetic coating layer on the surface of magnetic core changed the uniformity or magnitude of magnetization due to quenching of surface moments. However, the magnetization of the catalyst was still sufficient to respond to an external magnetic field.

The morphology and size of the nanoparticles were obtained from field emission scanning electron microscopy (FE-SEM) and transmission electron microscopy (TEM) analysis (Fig. S5). The images obtained at different magnifications demonstrated that the prepared magnetic nanoparticles are spherical in shape, with slight agglomeration.

In the EDX spectrum of the nanocatalyst (Fig. S6), the presence of Fe, Si and O signals indicates that the Fe_3O_4 nanoparticles are loaded with silica. Figure S6 also reveals the presence of the elemental composition of *N*-amidinoglycine (C, N and O) and palladium on the surface of the nanocatalyst.

Catalysis of Suzuki cross-coupling

In order to explore the catalytic activity of the present Pd nanocatalyst in the Suzuki reaction, we employed the coupling of 4-bromoacetophenone with phenylboronic acid as a model system to optimize the reaction conditions. The best results were obtained using water as the solvent and $NaHCO_3$ as the base, with 0.001 g of nanocatalyst (0.17 mmol% palladium) at 90 °C. As this catalyst is not sensitive to oxygen, the reactions were carried out under air (Table 1).

The scope and efficiency of this approach were then investigated for the synthesis of a wide variety of biaryl derivatives under the optimized conditions. The results are summarized in Table 2. Various aryl halides were tested, including either electron-donating or electron-withdrawing substituents such as Me, OMe, CN, NO_2, CHO, COMe and Cl. Also, both electron-rich and electron-deficient aryl boronic acids with Me, OMe, COMe and F substituents were utilized. As evident from Table 2, all the examined aryl iodides and bromides were successfully coupled with various phenylboronic acids, affording the corresponding products with good to excellent yields in short reaction times. Prolonged reaction times were required for the less active aryl chlorides to obtain the desired products in moderate yields.

A hot filtration test was also carried out, in order to demonstrate the absence of homogeneous catalytic species which is produced via leaching phenomena during the reaction. An mixture of 0.001 g of the Fe_3O_4@SiO_2@*N*-amidinoglycine@Pd^0 catalyst and $NaHCO_3$ (2 mmol) in 3 mL water was prepared and left to stir at 90 °C for 30 min, and then, the catalyst was magnetically removed. The filtrate so obtained showed negligible catalytic activity for Suzuki cross-coupling under the optimized reaction conditions (Table 3).

To study the recyclability of this palladium catalyst, we carried out a set of experiments using the recycled catalyst for the coupling of 4-bromoacetophenone with

Table 1 Optimization of reaction conditions in Suzuki cross-coupling reaction[a]

Entry	Solvent	Base	Time (min)	*T* (°C)	Catalyst (g)	Conversion (%)[b]
1	H_2O	Na_2CO_3	10	r.t	0.005	10
2	H_2O	Na_2CO_3	10	90	0.005	100
3	EtOH	Na_2CO_3	30	60	0.005	40
4	PEG	Na_2CO_3	10	100	0.005	10
5	H_2O	K_2CO_3	10	90	0.005	100
6	H_2O	$KHCO_3$	10	90	0.005	85
7	H_2O	$NaHCO_3$	10	90	0.005	100
8	H_2O	NaOAc	10	90	0.005	50
9	H_2O	KOH	10	90	0.005	85
10	H_2O	K_2CO_3	5	90	0.005	90
11	H_2O	Na_2CO_3	5	90	0.005	95
12	H_2O	$NaHCO_3$	5	90	0.005	100
13	H_2O	$NaHCO_3$(1 eq)	5	90	0.005	80
14	H_2O	$NaHCO_3$	5	90	0.01	100
15	H_2O	$NaHCO_3$	5	90	0.003	100
16	H_2O	$NaHCO_3$	5	90	0.001	100

[a]Reaction conditions: 4-bromoacetophenone (1 mmol), phenylboronic acid (1.2 mmol), base (2 mmol), Fe3O4@SiO2@*N*-amidinoglycine@Pd0 catalyst, solvent (3 mL)

[b]GC (*n*-hexane as internal standard) and TLC(*n*-hexane or *n*-hexane:ethylacetate 9:1) conversion

Table 2 Suzuki cross-coupling reactions using Fe_3O_4@SiO_2@*N*-amidinoglycine@Pd^0 nanocatalyst

Entry	Ar-X	Ar′B(OH)$_2$	Ar–Ar′	Time min	Yield[a] (%)
1	PhBr	PhB(OH)$_2$	Ph–Ph	10	96
3	*p*-OHC-PhBr	PhB(OH)$_2$	*p*-OHC-Ph–Ph	2	98
4	*p*-MeOC-PhBr	PhB(OH)$_2$	*p*-MeOC-Ph–Ph	5	98
5	*p*-NC-PhBr	PhB(OH)$_2$	*p*-NC-Ph–Ph	10	98
6	*p*-MeOPhI	PhB(OH)$_2$	*p*-MeO-Ph–Ph	10	97
7	PhBr	*p*-Me-PhB(OH)$_2$	*p*-Me-Ph–Ph	10	97
8	*p*-OHC-PhBr	*p*-Me-PhB(OH)$_2$	*p*-Me-Ph–Ph-*p*-CHO	10	98
9	*p*-MeOC-PhBr	*p*-Me-PhB(OH)$_2$	*p*-Me-Ph–Ph–*p*-COMe	10	98
10	*p*-NC-PhBr	*p*-Me-PhB(OH)$_2$	*p*-Me-Ph–Ph-*p*-CN	10	96
11	*m*-O_2N-PhI	*p*-Me-PhB(OH)$_2$	*p*-Me-Ph–Ph-*m*-NO_2	10	98
12	*p*-MeOC-PhBr	*p*-MeOC-PhB(OH)$_2$	*p*-MeOC-Ph–Ph-*p*-COMe	10	95
13	*p*-OHC-PhBr	*p*-MeOC-PhB(OH)$_2$	*p*-MeOC-Ph–Ph-*p*-CHO	10	95
14	*p*-MeO-PhI	*p*-MeOC-PhB(OH)$_2$	*p*-MeOC-Ph–Ph-*p*-OMe	10	96
15	*p*-Me-PhI	*p*-MeOC-PhB(OH)$_2$	*p*-MeOC-Ph–Ph-*p*-Me	10	98
16	*p*-MeO-PhI	*m*-MeO-PhB(OH)$_2$	*m*-MeO-Ph--Ph-*p*-OMe	10	97
17	*m*-O_2N-PhI	*m*-MeO-PhB(OH)$_2$	*m*-MeO-Ph–Ph-*m*-NO_2	10	93
18	*p*-MeOC-PhBr	*m*-MeO-PhB(OH)$_2$	*m*-MeO-Ph–Ph-*p*-COMe	10	96
19	*p*-MeOC-PhBr	3,4,5-F-PhB(OH)$_2$	3,4,5-F-Ph–Ph-*p*-COMe	10	98
20	*p*-OHC-PhBr	3,4,5-F-PhB(OH)$_2$	3,4,5-F-Ph–Ph-*p*-CHO	10	93
21	*p*-NC-PhCl	*p*-Me-PhB(OH)$_2$	*p*-Me-Ph–Ph-*p*-CN	90	50
22	*p*-NC-PhCl	PhB(OH)$_2$	*p*-NC-Ph–Ph	90	35

Reactions conditions: aryl halide (1 mmol), arylboronic acid (1 mmol), NaHCO3 (2 mmol), Fe3O4@SiO2@N-Amidinoglycine@Pd0 nanocatalyst (0.17 mmol%), H2O (3.0 mL), 90 °C, 10 min

[a]Isolated yields

Table 3 Reusability experiment of Fe_3O_4@SiO_2@*N*-amidinoglycine@Pd^0 catalyst

Run	Time (min)	Yield (%)
1	5	98
2	10	95
3	10	90
4	15	90

phenylboronic acid under the optimized conditions. After the completion of the first reaction, the catalyst was recovered magnetically, washed with ethanol, and dried for the next run. Then, a further reaction was carried out with fresh reactants and solvent under the same conditions. Based on the results, the catalyst retained its activity quite well over four successive catalytic runs, albeit with slightly longer reaction times.

We have compared the efficiency of Fe_3O_4@SiO_2@*N*-amidinoglycine@Pd^0 with previously reported catalysts for the synthesis of biphenyls to show the merits of the present work (Table 4). The results obtained with this catalytic system are superior to those for the other systems, giving better yields in shorter times with lower loading of palladium catalyst under mild reaction conditions.

Experimental

All reagents and solvents were purchased from commercial suppliers (Acros, Merck and Aldrich) and used without any additional purification. FT IR spectra were recorded using a Bruker Tensor 27 spectrometer within the 400–4000 cm^{-1} range using KBr disks. ^1H and ^{13}C NMR spectra were recorded with a Bruker Avance 400 and 100 MHz spectrometer using $CDCl_3$ as solvent and TMS as standard. XRD patterns were recorded with a PW 3710 X-ray diffractometer (Philips) at room temperature using monochromatic Cu Kα radiation with a wavelength of $\lambda = 0.15418$ nm. The peak positions and intensities were obtained between 5° and 80° with a rate of 0.04° s^{-1}. The morphology of the catalyst was observed with FE-SEM (HITACHI (S4160) Japan) and TEM (PHILIPS CM30) instruments. EDX patterns were recorded using a TESCAN, VEGA 3 LMU instrument. Magnetic susceptibility measurements were taken using a vibrating sample magnetometer (VSM, MDK Co. Ltd, Iran) with a magnetic field range of + 10,000 to − 10,000 Oe at room temperature. Elemental analyses were obtained on an

Table 4 Comparison of Fe_3O_4@SiO_2@*N*-amidinoglycine@Pd^0 with other catalysts in Suzuki cross-coupling

Reaction	Catalyst + conditions	Time	Yield (%)	References
p-CN-PhBr + $PhB(OH)_2$	γ-Fe_2O_3-acetamidine-Pd DMF, 100 °C	2 h	92	[28]
p-CN-PhBr + $PhB(OH)_2$	Fe_3O_4@SiO_2@L-arginine@Pd^0 (1.4 mmol% Pd),PEG, 100 °C	30 min	98	[29]
p-CN-PhBr + $PhB(OH)_2$	Fe_3O_4@SiO_2@*N*-amidinoglycine@Pd^0 (0.17 mmol%), H_2O, 90 °C	10 min	98	This work
p-MeOC-PhBr + $PhB(OH)_2$	Chitosan biguanidine/Pd (0.15 mol% Pd), EtOH–H_2O (1:1), 40 °C	2 h	90	[30]
p-MeOC-PhBr + $PhB(OH)_2$	Pd/Fe_3O_4@PMAA-Met (0.01 mol% Pd), EtOH–H_2O (1:1), 70 °C	30 min	98	[31]
p-MeOC-PhBr + $PhB(OH)_2$	SiO_2-NICOT-Pd^{II} (0.1 mol% Pd), EtOH–H_2O (1:1), 80 °C	2 h	97	[32]
p-MeOC-PhBr + $PhB(OH)_2$	Fe_3O_4@SiO_2@*N*-amidinoglycine@Pd^0 (0.17 mmol%), H_2O, 90 °C	5 min	98	This work

Eager 300 for EA1112 CHNS instrument. X-ray photoelectron spectroscopy (XPS) measurements were taken with a Thermo Scientific, ESCALAB 250 Xi Mg X-ray instrument.

Synthesis of Fe_3O_4@SiO_2

Magnetic nanoparticles (MNPs) were prepared by a conventional co-precipitation method. A mixture of $FeCl_3{\cdot}6H_2O$ (5.84 g, 22 mmol) and $FeCl_2{\cdot}4H_2O$ (2.15 g, 11 mmol) was dissolved in deionized water (100 mL) under a nitrogen atmosphere. The mixture was stirred vigorously at 85 °C for 30 min; then, ammonia solution (25 wt%, 10 mL) was added. The color of the solution changed immediately from orange to black. The black magnetite precipitate was collected with a magnet, washed twice with deionized water and then with 0.02 M NaCl solution and finally dried at 80 °C for 10 h.

The obtained Fe_3O_4 MNPs were subsequently coated with silica through the well-known Stöber method. Fe_3O_4 MNPs (1.0 g) were dispersed by ultrasonic vibration in a mixture of ethanol (40 mL), deionized water (6 mL) and aqueous ammonia solution (NH_3, 25 wt%, 3 mL), followed by the addition of tetraethylorthosilicate (1.4 mL). After stirring for 12 h at room temperature under an N_2 atmosphere, the black precipitate was collected using a magnet. The resulting Fe_3O_4@SiO_2 nanoparticles were washed several times with water and ethanol, and then dried at 80 °C for 10 h.

Synthesis of the nanocatalyst

Fe_3O_4@SiO_2 (1 g) was suspended in deionized water (40 mL) and sonicated until highly dispersed. *N*-Amidinoglycine (1.35 g) was then added to the mixture, which was stirred at 90 °C for 15 h. The resulting Fe_3O_4@SiO_2@*N*-amidinoglycine nanoparticles were separated by applying an external magnet, washed with distilled water several times and then dried in an oven overnight. Finally, incorporation of palladium onto the synthesized nanocomposite was carried out by mixing Fe_3O_4@SiO_2@*N*-amidinoglycine (0.5 g) and $Pd(OAc)_2$ (0.03 g) in absolute ethanol (30 mL). The mixture was refluxed for 24 h. The resulting Fe_3O_4@SiO_2@*N*-amidinoglycine@Pd^0 nanocatalyst was separated magnetically, washed with absolute ethanol and dried at room temperature.

General Suzuki coupling procedure

To a round-bottomed flask containing a mixture of aryl halide (1 mmol), arylboronic acid (1 mmol) and $NaHCO_3$ (2 mmol) in H_2O (3 ml), Fe_3O_4@SiO_2@*N*-amidinoglycine@Pd^0 catalyst (0.001 g, 0.017 mmol% Pd) was added, and the mixture was stirred at 90 °C for the time specified in Table 2. After completion of the reaction [monitored by TLC (*n*-hexane:EtOAc, 9:1) or GC], the mixture was cooled to room temperature and the catalyst was separated with an external magnet. The decantate was diluted with water and extracted with *n*-hexane to isolate the products. The combined organic layers were dried over $CaCl_2$, and the solvent was evaporated under reduced pressure. The residue was purified by silica gel column chromatography (*n*-hexane:EtOAc, 9:1).

Conclusion

In conclusion, we have demonstrated the Suzuki cross-coupling reaction in water using a highly efficient and green Fe_3O_4@SiO_2@*N*-amidinoglycine@Pd^0 catalyst. The generation of palladium nanoparticles without the addition of any

external reducing agent in the catalyst synthesis process, stability toward air and humidity, use of low catalyst loadings, easy handling and recyclability are the main advantages of this catalytic system. This catalyst was found to tolerate a broad range of functional groups. We hope that this heterogeneous magnetic nanocatalyst will find applications in palladium-catalyzed reactions.

Acknowledgements We gratefully acknowledge the partial financial support received from the research council of Alzahra University.

References

1. Lim CW, Lee IS (2010) Nano Today 5:412–434
2. Polshettiwar V, Luque R, Fihri A, Zhu H, Bouhrara M, Basset JM (2011) Chem Rev 111:3036–3075
3. Shylesh S, Schünemann V, Thiel WR (2010) Angew Chem Int Ed 49:3428–3459
4. Tang T, Fan H, Ai S, Han R, Qiu Y (2011) Chemosphere 83:255–264
5. Hu B, Pan J, Yu HL, Liu JW, Xu JH (2009) Process Biochem 44:1019–1024
6. Gupta AK, Gupta M (2005) Biomaterials 26:3995–4021
7. Ln Wu, Yang CY, Lv Z, Cui FW, Zhao L, Yang P (2015) RSC Adv 5:50557–50564
8. Ahmadi R, Ranjbarnodeh E, Gu N (2012) Mater Sci Poland 30:382–389
9. Balu AM, Baruwati B, Serrano E, Cot J, Garcia-Martinez J, Varma RS, Luque R (2011) Green Chem 13:2750–2758
10. Deng Y, Cai Y, Sun Z, Zhao D (2011) Chem Phys Lett 510:1–13
11. Lu AH, Salabas EL, Schüth F (2007) Angew Chem Int Ed 46:1222–1244
12. Chekina N, Horak D, Jendelova P, Trchova M, Benes MJ, Hruby M, Herynek V, Turnovcova K, Sykova E (2011) J Mater Chem 21:7630–7639
13. Yang J, Lee J, Kang J, Chung CH, Lee K, Suh JS, Yoon HG, Huh YM, Haam S (2008) Nanotechnology 19:075610
14. Stöber W, Fink A, Bohn EJ (1968) J Colloid Interface Sci 26:62–69
15. Lu Y, Yin Y, Mayers BT, Xia Y (2002) Nano Lett 2:183–186
16. Graf C, Vossen DLJ, Imhof A, Van Blaaderen A (2003) Langmuir 19:6693–6700
17. Qu H, Maa H, Zhou W, O'Connor CJ (2012) Inorg Chim Acta 389:60–65
18. Ebrahiminezhad A, Ghasemi Y, Rasoul-Amini S, Barar J, Davaran S (2013) Colloids Surf B Biointerfaces 102:534–539
19. Wang Z, Zhu H, Wang X, Yang F, Yang X (2009) Nanotechnology 20:465606–465615
20. Miyaura N, Suzuki A (1995) Chem Rev 95:2457–2483
21. Bringmann G, Gulder T, Gulder TAM, Breuning M (2011) Chem Rev 111:563–639
22. Wencel-Delord J, Panossian A, Leroux FR, Colobert F (2015) Chem Soc Rev 44:3418–3430
23. Meyer FM, Collins JC, Borin B, Bradow J, Liras S, Limberakis C, Mathiowetz AM, Philippe L, Price D, Song K, James K (2012) J Org Chem 7:3099–3114
24. Kappaun S, Slugovc C, List EJW (2008) Int J Mol Sci 9:1527–1547
25. Polshettiwar V, Decottignies A, Len C, Fihri A (2010) Chem Sus Chem 3:502–522
26. Chatterjee A, Ward TR (2016) Catal Lett 146:820–840
27. Liu X, Ma Z, Xing J, Liu H (2004) J Magn Magn Mater 270:1–6
28. Sobhani S, Ghasemzadeh MS, Honarmand M, Zarifi F (2014) RSC Adv 4:44166–44174
29. Ghorbani-Choghamarani A, Azadi G (2016) Appl Organomet Chem 30:247–252
30. Veisi H, Ghadermazi M, Naderi A (2016) Appl Organomet Chem 30:341–345
31. Yang P, Ma R, Bian F (2016) ChemCatChem 18:3746–3754
32. Hajipour AR, Tadayoni NS, Mohammadsaleh F (2016) Appl Organomet Chem 30:777–782